PHYSICAL REVIEW D **80,** 094011 (2009)

Multichannel calculation of excited vector ϕ resonances and the $\phi(2170)$

Susana Coito* and George Rupp†

Centro de Física das Interacções Fundamentais, Instituto Superior Técnico, Technical University of Lisbon, P-1049-001 Lisboa, Portugal

Eef van Beveren‡

Centro de Física Computacional, Departamento de Física, Universidade de Coimbra, P-3004-516 Coimbra, Portugal

(Received 7 September 2009; revised manuscript received 11 October 2009; published 16 November 2009)

A multichannel calculation of excited $J^{PC} = 1^{--}$ ϕ states is carried out within a generalization of the resonance-spectrum expansion, which may shed light on the classification of the $\phi(2170)$ resonance, discovered by *BABAR* and originally denoted $X(2175)$. In this framework, a complete spectrum of bare $s\bar{s}$ states is coupled to those Okubo-Zweig-Iizuka–allowed decay channels that should be most relevant for the considered energy range. The included S- and P-wave two-meson channels comprise the lowest pseudoscalar, vector, scalar, and axial-vector mesons, while in the $q\bar{q}$ sector both the $^3S_1$ and $^3D_1$ states are coupled. The only two free parameters are tuned so as to reproduce mass and width of the $\phi(1020)$, but come out reasonably close to previously used values. Among the model's T-matrix poles, there are good candidates for observed resonances, as well as other ones that should exist according to the quark model. Besides the expected resonances as unitarized confinement states, a dynamical resonance pole is found at $(2186 - i246)$ MeV. The huge width makes its interpretation as the $\phi(2170)$ somewhat dubious, but further improvements of the model may change this conclusion.

DOI: 10.1103/PhysRevD.80.094011 PACS numbers: 14.40.Cs, 11.55.Ds, 11.80.Gw, 13.75.Lb

I. INTRODUCTION

In 2006, the *BABAR* Collaboration announced [1] the discovery of a new vector-meson resonance, called $X(2175)$, in the initial-state-radiation process $e^+e^- \to K^+K^-\pi\pi\gamma$, observed in the channel $\phi(1020)f_0(980)$, with the ϕ meson decaying to K^+K^- and the $f_0(980)$ to $\pi^+\pi^-$ or $\pi^0\pi^0$. Two years later, the BES Collaboration confirmed [2] this resonance, then denoted $Y(2175)$, in the decay $J/\psi \to \eta[\to \gamma\gamma]\phi[\to K^+K^-]f_0(980)[\to \pi^+\pi^-]$. At present, the new state is included in the PDG listings as the $\phi(2170)$ [3], though not in the summary table, with average mass $M = (2175 \pm 15)$ MeV and width $\Gamma = (61 \pm 18)$ MeV. However, these resonance parameters are being strongly challenged by the very recent Belle [4] results on the $Y(2175)$, alias $\phi(2170)$, observed in the process $e^+e^- \to \phi\pi^+\pi^-$, yielding $M = (2079 \pm 13^{+79}_{-28})$ MeV and $\Gamma = (192 \pm 23^{+25}_{-61})$ MeV.

The observation of this highly excited ϕ-type resonance with (probably) modest width, besides the peculiar, seemingly preferential, decay mode $\phi f_0(980)$, triggered a variety of model explications, most of which propose exotic solutions. Let us mention first a strangeonium-hybrid $(s\bar{s}g)$ assignment, in the flux tube as well as the constituent-gluon model [5], and a perturbative comparison of $\phi(2170)$ decays in these exotic *Ansätze* with a standard 2^3D_1 $s\bar{s}$ description from both the flux tube and the $^3P_0$ model, by the same authors [6]. Other approaches in terms of exotics, with QCD sum rules, are an $ss\bar{s}\bar{s}$ tetraquark assignment [7], and an analysis [8] exploring both $ss\bar{s}\bar{s}$ and $s\bar{s}s\bar{s}$ configurations. In an effective description based on resonance chiral perturbation theory [9], the bulk of the experimental data is reproduced except for the $\phi(2170)$ peak. This then led to a 3-body Faddeev calculation [10], with the pair interactions taken from the chiral unitary approach. Indeed, a resonance with parameters reasonably close to those of the $\phi(2170)$ is thus generated, though a little bit too narrow. Finally, a review on several puzzling hadron states [11] mentions the possibility that the $\phi(2170)$ arises from S-wave threshold effects.

In the present paper, we shall study the possibility that the $\phi(2170)$ is a normal excited ϕ meson, by coupling a complete confinement spectrum of $s\bar{s}$ states to a variety of S- and P-wave two-meson channels, composed of pairs of ground-state pseudoscalar (P), vector (V), scalar (S), and axial-vector (A) mesons. The employed formalism is a multichannel generalization of the resonance-spectrum expansion (RSE) [12,13], which allows for an arbitrary number of confined and scattering channels [14].

In Sec. II the RSE is very briefly reviewed and the explicit T matrix for the present coupled-channel system is given. Resonance poles and their trajectories are shown in Sec. III, and model cross sections in Sec. IV. We draw our conclusions in Sec. V and discuss possible improvements.

II. THE RSE APPLIED TO ϕ RECURRENCES

The RSE model has been developed for meson-meson scattering in nonexotic channels, whereby the intermediate

*susana.coito@ist.utl.pt
†george@ist.utl.pt
‡eef@teor.fis.uc.pt

state is described via an infinite tower of s-channel $q\bar{q}$ states. For the spectrum of the latter, in principle any confinement potential can be employed, but in practical applications, a harmonic oscillator (HO) with constant frequency has been used, with excellent results. For more details and further references, see Refs. [12,13,15–18].

In the present investigation of strangeonium vector mesons, both the $^3S_1$ and $^3D_1$ $s\bar{s}$ confinement channels are included, to be compared with recent work [19] restricted to the $^3S_1$ component only. We could in principle also consider deviations from ideal mixing, by coupling the corresponding two $(u\bar{u} + d\bar{d})/\sqrt{2}$ channels as well, but such fine corrections will be left for possible future studies. For the meson-meson channels, we consider the most relevant combinations of ground-state P, V, S, and A mesons that have nonvanishing coupling to either of the two confinement channels in accordance with the $^3P_0$ model and the Okubo-Zweig-Iizuka (OZI) rule. The resulting 17 channels are listed, with all their relevant quantum numbers, in Table I. For the channels containing an η or η' meson, we assume a pseudoscalar mixing angle of 37.3°, in the flavor basis, though our results are not very sensitive to the precise value. Also note that channels with the same particles but different relative orbital angular momentum L or total spin S are considered different. This is only strictly necessary for different L, because of the corresponding wave functions, but is also done when S is different, for the purpose of clarity. All relative couplings have been computed using the formalism of Ref. [20], based on overlaps of HO wave functions. They are given in Table I for the lowest recurrences ($n = 0$). As a matter of fact, we list their squares, which are rational numbers, but given as rounded floating-point numbers in the table, also for clarity's sake. For higher n values, the couplings fall off very rapidly. Their n dependence, for the various sets of decay channels, is presented in Table II. The threshold values in Table I are obtained by taking the meson masses given in the PDG tables or listings [3], with the exception of the $K_0^*(800)$ (alias κ), for which we choose the real part of the pole position from Ref. [16], as it lies closer to the world average of κ masses. Note that we take sharp thresholds, even when (broad) resonances are involved. We shall come back to this point in the Conclusions. Finally, we should notice that a number of channels that also couple to $s\bar{s}$ vector states according to the scheme of Ref. [20], viz. P-wave channels involving axial-vector mesons as well as some channels with tensor mesons, have not been included in the final calculations presented here. However, their influence has been tested and turned out to be very modest, due to the corresponding small couplings.

TABLE II. Dependence of couplings squared on recurrence n.

Channel	$\tilde{g}^2_{(l_c=0,n)} \times 4^n$	$\tilde{g}^2_{(l_c=2,n)} \times 4^n$
PP	$(2n+3)/3$	$n+1$
PV	$(2n+3)/3$	$n+1$
VV	$(2n+3)/3$	$n+1$
SV	$(2n-3)^2/9$	$(n+1)(2n+5)/5$
PA	$(2n-3)^2/9$	$(n+1)(2n+5)/5$
VA	$(2n-3)^2/9$	$(n+1)^2$

TABLE I. Included two-meson channels, their internal and relative angular momenta and spins, couplings squared for $n = 0$, and thresholds. See Ref. [3] for properties of listed mesons, except for the $K_0^*(800)$, discussed in the text.

Channel	$g^2_{(l_c=0)} \times 10^{-3}$	$g^2_{(l_c=2)} \times 10^{-3}$	l_1	l_2	L	S	Threshold (MeV)
KK	27.8	9.26	0	0	1	0	987
KK^*	111	9.26	0	0	1	1	1388
$\eta\phi$	40.8	3.40	0	0	1	1	1567
$\eta'\phi$	70.3	5.86	0	0	1	1	1977
K^*K^*	9.26	3.09	0	0	1	0	1788
K^*K^*	185	0.62	0	0	1	2	1788
$\phi(1020)f_0(980)$	83.3	0.0	0	1	0	1	1999
$K^*K_0^*(800)$	83.3	0.0	0	1	0	1	1639
$\phi(1020)f_0(980)$	0.0	14.7	0	1	2	1	1999
$K^*K_0^*(800)$	0.0	14.7	0	1	2	1	1639
$\eta h_1(1380)$	10.2	5.67	0	1	0	1	1928
$\eta' h_1(1380)$	17.6	9.76	0	1	0	1	2338
$KK_1(1270)$	83.3	20.6	0	1	0	1	1764
$KK_1(1400)$	0.0	2.57	0	1	0	1	1894
$K^*K_1(1270)$	167	10.3	0	1	0	1	2164
$K^*K_1(1400)$	0.0	1.29	0	1	0	1	2294
$\phi f_1(1420)$	111	3.86	0	1	0	1	2439

Coming now to the explicit expressions for our model, let us first write down the effective meson-meson interaction, which consists of an intermediate-state s-channel $q\bar{q}$ propagator between two quark-antiquark–meson-meson vertex functions for the initial and final state, reading [13,14]

$$V_{ij}^{L_i,L_j}(p_i, p'_j; E) = \lambda^2 j^i_{L_i}(p_i a)\mathcal{R}_{ij}(E) j^j_{L_j}(p'_j a), \quad (1)$$

with

$$\mathcal{R}_{ij}(E) = \sum_{l_c=0,2}\sum_{n=0}^{\infty}\frac{g^i_{(l_c,n)}g^j_{(l_c,n)}}{E - E_n^{(l_c)}}, \quad (2)$$

where the RSE propagator contains an infinite tower of s-channel bare $q\bar{q}$ states, corresponding to the spectrum of an, in principle, arbitrary confining potential. Here, $E_n^{(l_c)}$ is the discrete energy of the nth recurrence in the $s\bar{s}$ channel with angular momentum l_c, and $g^i_{(l_c,n)}$ is the corresponding coupling to the ith meson-meson channel. Furthermore, in Eq. (1), λ is an overall coupling, and $j^i_{L_i}(p_i)$ and p_i are the L_ith order spherical Bessel function and the (relativistically defined) off-shell relative momentum in meson-meson channel i, respectively. The spherical Bessel function originates in our string-breaking picture of OZI-allowed decay, being just the Fourier transform of a spherical delta function of radius a. Together with the overall coupling constant λ, the radius a is a freely adjustable parameter here, though its range of allowed values turns out to be quite limited in practice. The couplings $g^i_{(l_c,n)}$ in Eq. (2) are obtained by multiplying the ones in Table I by those in Table II, for the corresponding channels. Because of the fast decrease of the latter for increasing n, practical convergence of the infinite sum in Eq. (2) is achieved by truncating it after 20 terms.

Because of the separable form of the effective meson-meson interaction in Eq. (1), the fully off-shell T matrix can be solved in closed form with straightforward algebra, resulting in the expression

$$T_{ij}^{(L_i,L_j)}(p_i, p'_j; E) = -2a\lambda^2\sqrt{\mu_i p_i} j^i_{L_i}(p_i a)\sum_{m=1}^{N}\mathcal{R}_{im} \times \{[1 - \Omega\mathcal{R}]^{-1}\}_{mj} j^j_{L_j}(p'_j a)\sqrt{\mu_j p'_j}, \quad (3)$$

with

$$\Omega_{ij}(k_j) = -2ia\lambda^2\mu_j k_j j^j_{L_j}(k_j a)h^{(1)j}_{L_j}(k_j a)\delta_{ij}, \quad (4)$$

where $h^{(1)j}_{L_j}(k_j a)$ is the spherical Hankel function of the first kind, k_j and μ_j are the on-shell relative momentum and reduced mass in meson-meson channel j, respectively, and the matrix $\mathcal{R}(E)$ is given by Eq. (2).

As mentioned above, we assume an HO confinement spectrum with constant frequency, given by

$$E_n = 2m_s + \omega(2n + l_c + 1.5), \quad (5)$$

TABLE III. Masses of bare $s\bar{s}$ states in MeV, for HO potential with $\omega = 190$ MeV and $m_s = 508$ MeV [see Eq. (5) and Ref. [21]].

n	$l_c = 0$	$l_c = 2$
0	1301	1681
1	1681	2061
2	2061	2441
3	2441	2821

with $\omega = 190$ MeV and $m_s = 508$ MeV fixed at values determined long ago [21]. Some of the resulting bare HO $s\bar{s}$ states are given in Table III.

Now that the model has been fully defined, we are in a position to evaluate the on-shell components of the T matrix defined in Eqs. (3) and (2), for the channels given in Tables I, II, and III.

III. EXPERIMENTAL STATUS OF ϕ STATES

Before adjusting our two free parameters λ and a from Eq. (3), let us first have a look at the experimental status of vector ϕ resonances. According to the 2008 PDG listings [3], there are only 3 observed states, viz. the $\phi(1020)$, $\phi(1680)$, and $\phi(2170)$, with the latter resonance omitted from the summary table. Their PDG masses and widths are given in Table IV. Clearly, this is a very poor status, as several additional states must exist in the energy range 1–2 GeV according to the quark model, and also if we compare with e.g. observed ρ resonances [3] in the same energy interval. Moreover, the $\phi(1680)$ can hardly be the first radial excitation of the $\phi(1020)$, in view of the well-established $K^*(1410)$, which is almost 300 MeV lighter, and a typical mass difference of 100–150 MeV between the strange and nonstrange (u, d) constituent quarks [21,22]. This conclusion is further supported if indeed the $\rho(1250)$ is confirmed as the first radial recurrence of the $\rho(770)$ [21,23]. So the $\phi(1680)$ is more likely to be the 1^3D_1 state, with a hitherto undetected 2^3S_1 state somewhere in the mass range 1.5–1.6 GeV. As a matter of fact, in Ref. [24] a vector ϕ resonance was reported at roughly 1.5 GeV, though this observation is, surprisingly, included under the $\phi(1680)$ entry [3]. Even more oddly, another ϕ-like state, at ~1.9 GeV and reported in the same paper [24], is *also* included under the $\phi(1680)$ [3]. However, a resonance at about 1.9 GeV should be a good candidate for the next radial $s\bar{s}$ recurrence, if we take the observed ρ resonances in Ref. [23] for granted.

TABLE IV. Listed $J^{PC} = 1^{--}$ ϕ resonances, with masses and widths [3] [values for $\phi(1680)$ are estimates [3]].

	M (MeV)	Γ (MeV)
$\phi(1020)$	1019.455 ± 0.020	4.26 ± 0.04
$\phi(1680)$	1680 ± 20	150 ± 50
$\phi(2170)$	$\mathbf{2175 \pm 15}$	$\mathbf{61 \pm 18}$

IV. HUNTING AFTER POLES

In view of the poor status of excited ϕ states, let us adjust our parameters λ and a to the mass and width of the $\phi(1020)$. Here, we should mention that an additional phenomenological ingredient of our model is an extra suppression of subthreshold contributions, using a form factor, on top of the natural damping due to the spherical Bessel and Hankel functions in Eq. (2). Such a procedure is common practice in multichannel phase-shift analyses. Thus, for closed meson-meson channels we make the substitution

$$(g^i_{(l_c,n)})^2 \to (g^i_{(l_c,n)})^2 e^{\alpha k_i^2} \quad \text{for } \mathrm{Re}k_i^2 < 0. \tag{6}$$

The parameter α is chosen at exactly the same value as in previous work [16,18], viz. $\alpha = 4\ \mathrm{GeV}^{-2}$.

Choosing now $\lambda = 4\ \mathrm{GeV}^{-3/2}$ and $a = 4\ \mathrm{GeV}^{-1}$, we manage to reproduce mass and width of the $\phi(1020)$ with remarkable accuracy, namely, $M_\phi = 1019.5$ MeV and $\Gamma_\phi = 4.4$ MeV. Note that these values of λ and a are of the same order of magnitude as in the work mentioned before [16,18], which dealt with scalar mesons.

In Table V we collect all resonance poles encountered on the respective physical Riemann sheets, which correspond to $\mathrm{Im}k_i > 0$ for closed channels and $\mathrm{Im}k_i < 0$ for open ones. When the latter conditions are not fulfilled, we call the corresponding Riemann sheets unphysical. Moreover, we also show here the pole positions obtained by taking only the $^3S_1$ $s\bar{s}$ channel and switching off the $^3D_1$, for fixed λ and a. Focusing for the moment on those poles that originate in the states of the confinement spectrum (indicated by "Conf." in the table), we see good candidates for the resonances at $\sim$1.5 and $\sim$1.9 GeV reported in Ref. [24], and possibly also for the $\phi(1680)$, though our 1^3D_1 state seems somewhat too light. Note, however, that under the $\phi(1680)$ entry [3] in the PDG listings there is a relatively recent observation [25] with a mass of (1623 ± 20) MeV, which is compatible with our pole at 1602 MeV. Furthermore, the imaginary parts of the confinement poles are generally too small, except for the $\phi(1020)$. We shall come back to this point in the Conclusions. Besides the latter poles, also two so-called *continuum* poles are found, often designated as *dynamical* poles, the most conspicuous of which is the one at $(2186 - i246)$ MeV, as the real part is very close to the mass of the $\phi(2170)$ as measured by *BABAR* [1] and BES [2]. However, in view of the much too large width, even as compared to the Belle [4] value, considerable caution is urged. Also this point will be further discussed in the Conclusions.

TABLE V. Complex-energy poles in MeV, for the $^3S_1$ $s\bar{s}$ channel only, and for both $^3S_1$ and $^3D_1$. See text for further details.

	$^3S_1$ only		$^3S_1 + {}^3D_1$		
Pole	Re	Im	Re	Im	Type of pole
1	1027.5	−2.7	1019.5	−2.2	Conf., $n = 0$, 1^3S_1
2	1537	−13	1516	−23	Conf., $n = 1$, 2^3S_1
3	⋯	⋯	1602	−6	Conf., $n = 0$, 1^3D_1
4	1998	−16	1932	−24	Conf. $n = 2$, 3^3S_1
5	⋯	⋯	1996	−14	Conf. $n = 1$, 2^3D_1
6	2397	−214	**2186**	**−246**	Continuum
7	2415	−6	2371	−29	Conf., $n = 3$, 4^3S_1
8	⋯	⋯	2415	−8	Conf., $n = 2$, 3^3D_1
9	2501	−236	2551	−193	Continuum

Some words are in place here about our identification of the $^3S_1$ and $^3D_1$ confinement poles in Table V. The point is that, rigorously speaking, these designations only make sense for pure confinement states and, moreover, without any $^3S_1/^3D_1$ mixing. Now, in our approach, the very mixing is provided by the coupling to common decay channels. So for any nonvanishing value of the overall coupling λ there are no longer pure $^3S_1$ and $^3D_1$ states, while for the physical value of λ the mixing is probably considerable. Moreover, there is no obvious way to tell which pole of a pair originating in a degenerate confinement state stems from either $^3S_1$ or $^3D_1$. Therefore, our identification is partly based on the couplings in Table I, which on the whole suggest larger shifts for $^3S_1$ than for $^3D_1$, partly on a comparison with a perturbative approach employed in Ref. [26] to find poles for small λ.

The designation continuum pole becomes clear when plotting a corresponding trajectory as a function of the

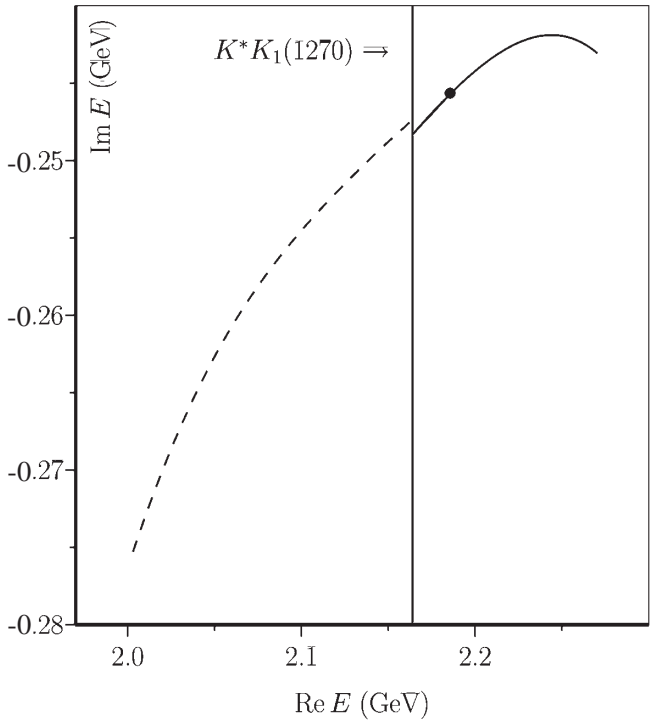

FIG. 1. Trajectory of first continuum pole, for $2.26 \le \lambda \le 5.99$ $(\mathrm{GeV}^{-3/2})$, from left to right. The bullet represents $\lambda = 4\ \mathrm{GeV}^{-3/2}$, while the dashed line indicates the unphysical Riemann sheet.

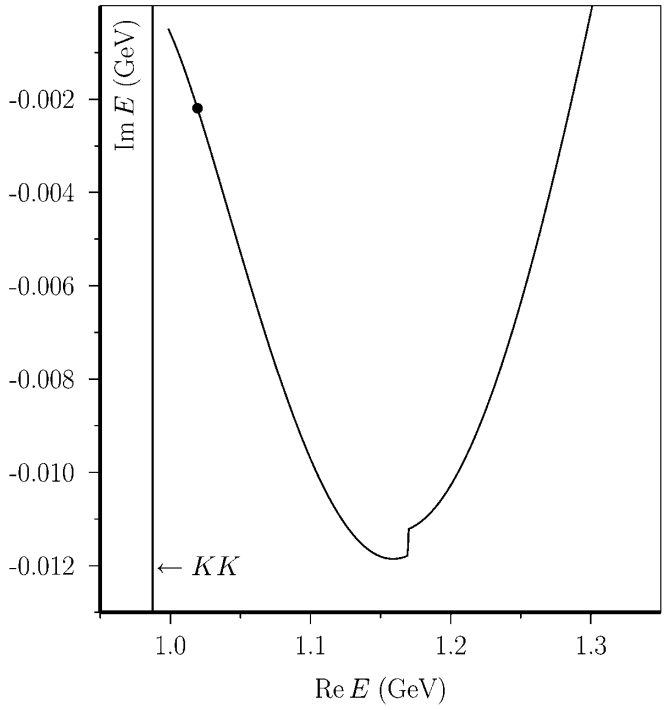

FIG. 2. 1^3S_1 confinement pole for $4.31 \geq \lambda \geq 0$ ($\mathrm{GeV}^{-3/2}$). The bullet represents $\lambda = 4$ $\mathrm{GeV}^{-3/2}$.

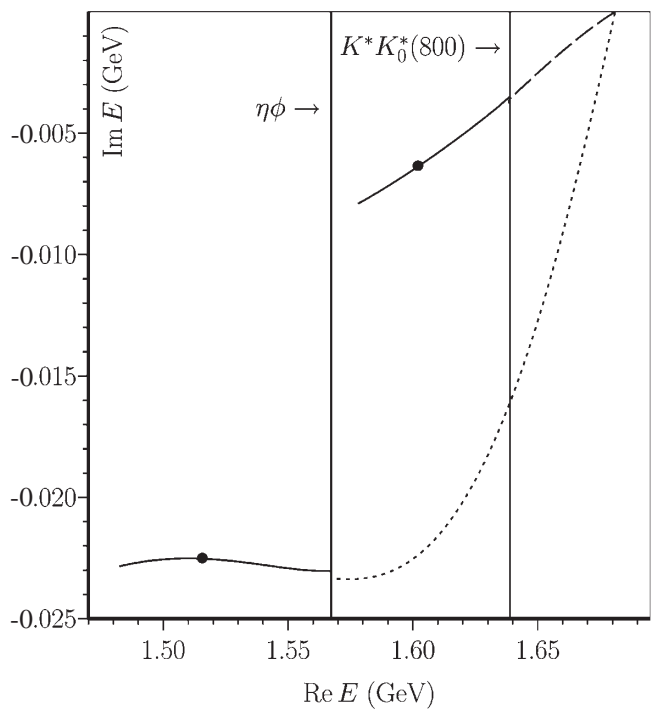

FIG. 3. 2^3S_1 (lower) and 1^3D_1 (upper) confinement poles for $5.0 \geq \lambda \geq 0$ ($\mathrm{GeV}^{-3/2}$) and $4.76 \geq \lambda \geq 0$ ($\mathrm{GeV}^{-3/2}$), respectively. The bullets represent $\lambda = 4$ $\mathrm{GeV}^{-3/2}$, while the dotted and dashed lines indicate unphysical Riemann sheets.

overall coupling λ. In Fig. 1, the first such pole is shown to have an *increasingly* large imaginary part for *decreasing* λ, eventually disappearing in the continuum for $\lambda \to 0$. Note that the small jump at the important S-wave $K^*K_1(1270)$ threshold is due to a minor threshold discontinuity of the damping function in Eq. (6) for complex momenta.

Figure 2 shows a similar trajectory, but now for the lowest confinement pole, which ends up as the $\phi(1020)$ resonance. Notice the large negative mass shift ($\approx$ 280 MeV), as well as the way the pole approaches the $K\bar{K}$ threshold, which is typical for P-wave decay channels. Also note that the tiny jump in the trajectory is due to the way relativistic reduced mass is defined below threshold, which in the case of closed channels with highly unequal masses [$KK_1(1270)$ here] requires an intervention to prevent the reduced mass from becoming negative.

In Fig. 3, we depict the trajectories of the 2^3S_1 and 1^3D_1 confinement poles. Note that the coupling to decay channels lifts the original degeneracy of the 2^3S_1 and 1^3D_1 HO states.

The trajectories of the next pair of confinement poles, i.e., 3^3S_1 and 2^3D_1, are drawn in Fig. 4. Note the highly nonlinear behavior of the poles, showing the unreliability of perturbative methods to estimate coupled-channel effects.

V. CROSS SECTIONS

Now we shall show, as mere illustrations, some of the cross sections related to the resonance poles found in the

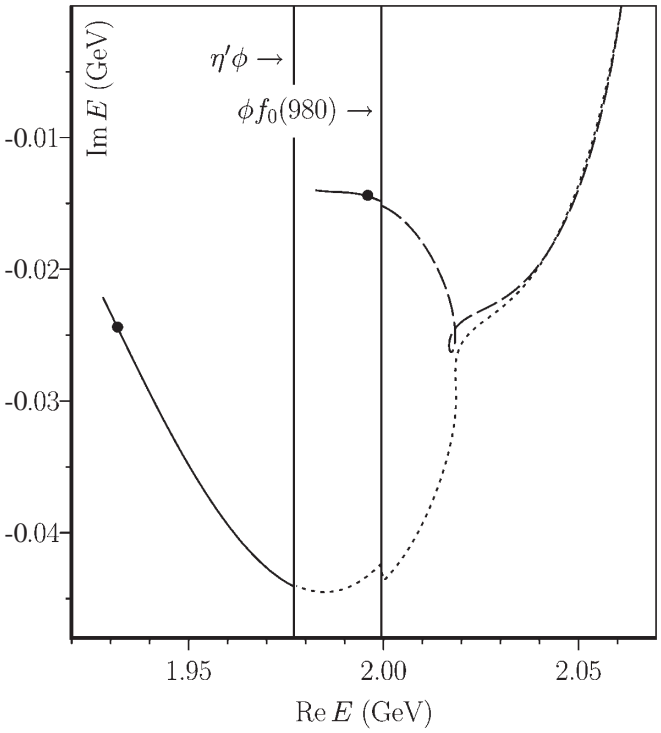

FIG. 4. 3^3S_1 (lower) and 2^3D_1 (upper) confinement poles for $4.2 \geq \lambda \geq 0$ ($\mathrm{GeV}^{-3/2}$) and $5.99 \geq \lambda \geq 0$ ($\mathrm{GeV}^{-3/2}$), respectively. The bullets represent $\lambda = 4$ $\mathrm{GeV}^{-3/2}$, while the dotted and dashed lines indicate unphysical Riemann sheets.

preceding section. In Fig. 5, the elastic P-wave KK cross section is depicted in the energy region covering the $\phi(1020)$ as well as the 2^3S_1 and 1^3D_1 resonances. We see that including the $^3D_1$ $s\bar{s}$ channel has the effect of lowering the 2^3S_1 state, besides the generation of an additional resonance, of course. This ''repulsion'' between the $^3S_1$ and $^3D_1$ poles is also noticed for the 3^3S_1 and 2^3D_1 states.

Figure 6 shows the relative importance of the KK and KK^* channels in the energy interval 1.5–1.7 GeV, which should be relevant for the $\phi(1680)$. The plotted quantity is the logarithm of the ratio of the elastic KK^* and KK cross sections, which shows that the KK^* channel is strongly dominant, except at low energies, because of phase space, and close to the pole at ~1.6 GeV, where the two cross sections are comparable. Dominance of the KK^* decay mode is reported under the $\phi(1680)$ PDG entry [3].

Turning now to the $\phi(2170)$ energy region, we show in Fig. 7 the elastic S- and D-wave $\phi(1020)f_0(980)$ cross sections. The effect of the continuum pole at $(2186 - i246)$ MeV is noticeable as a small and very broad enhancement in the D-wave cross section. In the S-wave case, its effect is completely overwhelmed by the huge cross section at threshold, partly due to the 3^3S_1 pole not far below. Also quite conspicuous are the here predicted 4^3S_1 and 3^3D_1 resonances (see Table V for the respective pole positions). Of course, all of these model *elastic* cross sections have little direct bearing upon the experimentally observed *production* cross sections. The production process of the $\phi(2170)$ may be studied with the RSE produc-

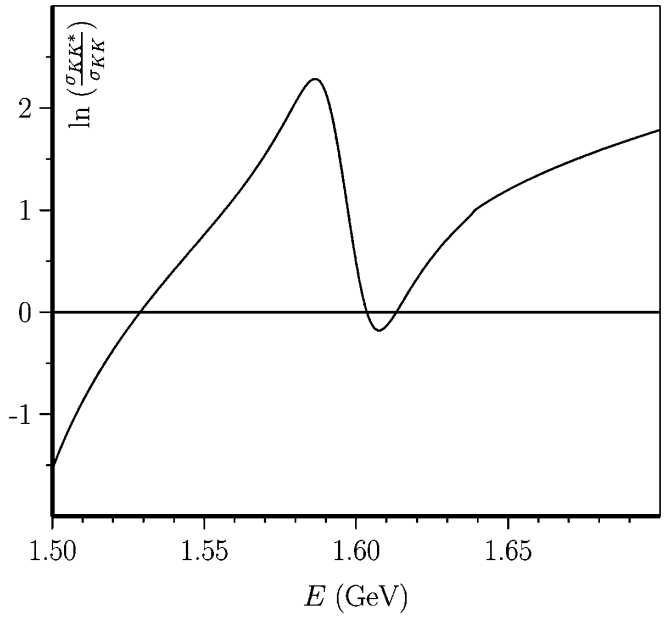

FIG. 6. Natural logarithm of the ratio of the elastic KK^* and KK cross sections.

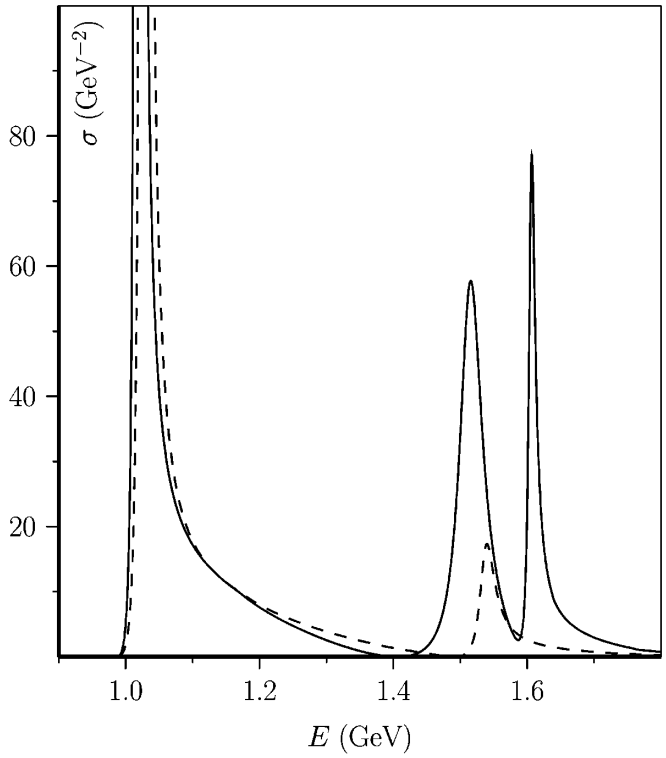

FIG. 5. Elastic P-wave KK cross section. Solid line: both $^3S_1$ and $^3D_1$ $s\bar{s}$ channels included; dashed line: only $^3S_1$.

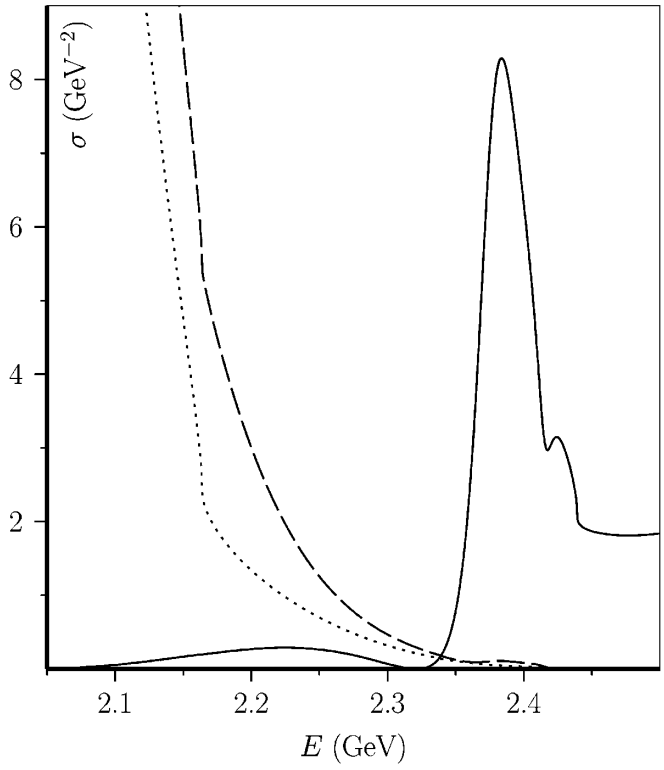

FIG. 7. Elastic D-wave (solid line) and S-wave (dashed line) $\phi(1020)f_0(980)$ cross sections. Dotted line: S-wave cross section for the $^3S_1$ channel only.

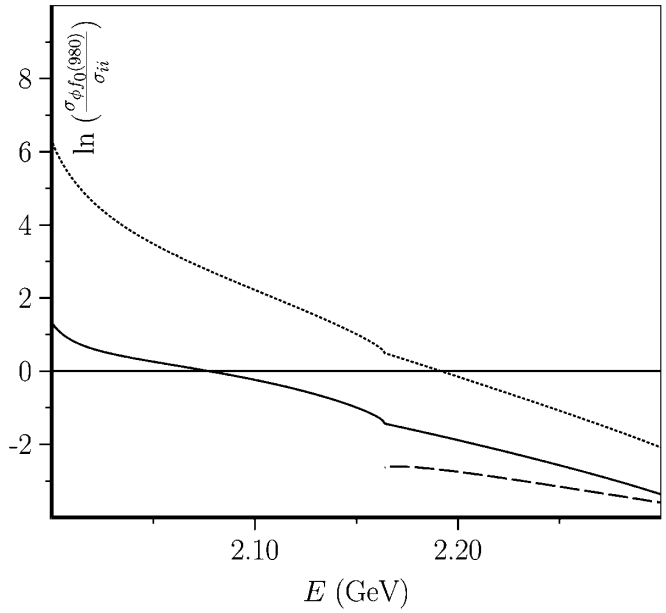

FIG. 8. Natural logarithm of the ratios of the elastic S-wave $\phi(1020)f_0(980)$ cross section and the elastic K^*K^* (solid line), $\phi(1020)\eta'$ (dotted line), and $K^*K_1(1270)$ (dashed line) cross sections.

tion formalism [27], but that lies outside the scope of the present investigation, which focused on the possibility of generating a $\phi(2170)$ resonance pole through coupled channels.

Finally, in Fig. 8 we plot the logarithm of the ratios of the elastic S-wave $\phi(1020)f_0(980)$ cross section and the elastic K^*K^*, $\phi(1020)\eta'$, and $K^*K_1(1270)$ cross sections, in the energy interval 2.0–2.3 GeV. We see that the S-wave $\phi(1020)f_0(980)$ cross section dominates up to about 2.08 GeV, but getting overwhelmed first by the (P-wave) K^*K^* channel, and then even more so by the S-wave $K^*K_1(1270)$ channel, right from its threshold at $\approx$ 2.16 GeV upward. Also the $\phi(1020)\eta'$ channel is becoming more important here. As for the K^*K^* channel, it gives rise to a final state with two kaons and two pions, i.e., the same as that for which the $\phi(2170)$ was observed. So the experimental status of the $\phi(2170)$ might be improved if one succeeded in identifying and isolating the $K^*[\rightarrow K\pi]K^*[\rightarrow K\pi]$ decay mode, which should be quite important.

VI. SUMMARY AND CONCLUSIONS

In this paper, we have applied the RSE formalism for nonexotic multichannel meson-meson scattering to calculate the resonance spectrum of excited vector ϕ mesons, and to find out whether this way the $\phi(2170)$ can be generated. The inclusion of all relevant two-meson channels that couple to the bare $^3S_1$ and $^3D_1$ $s\bar{s}$ states should guarantee a reasonable description. Thus, several vector ϕ resonances are predicted, some of which are good candidates for observed states, while others may correspond to others, undetected so far, but quite plausible in view of observed partner states in the excited ρ spectrum. Finally, a very broad ϕ-like resonance pole of a dynamical origin is found, with real part very close to that of the $\phi(2170)$, but a much too large imaginary part, so that its interpretation remains uncertain. On the other hand, the calculated resonances originating in the confinement spectrum are generally too narrow.

These considerations bring us to the main problem of our description, namely, the inclusion of sharp thresholds only. The point is that many of the channels in Table I involve highly unstable particles, several of which are broad to very broad resonances themselves. Treating the corresponding thresholds as sharp is clearly an approximation. In particular, the $f_0(980)$ meson included in the $\phi(1020)f_0(980)$ channels is a very pronounced resonance in the coupled $\pi\pi$-KK system. This feature is crucial in the three-body calculation of the $\phi(2170)$ in Ref. [10], which indeed produces a clear resonance signal at almost the right energy, and even with a somewhat too *small* width. We believe that in our approach, too, a narrower $\phi(2170)$ might be generated, if we could account for the physical width of the $f_0(980)$ meson, and also for the widths of the K^* and $K_1(1270)$ resonances in the here included $K^*K_1(1270)$ channel. The reason is that the widths effectively cause these channels to act already below their central thresholds, which will strongly influence poles just underneath. Especially the width of the very strongly coupling $K^*K_1(1270)$ channel, whose threshold lies only some 25 MeV below the real part of the continuum pole at $(2186 - i \times 246)$ MeV, will surely have a very significant effect on this pole's trajectory. Because of the typical behavior of continuum poles, with decreasing width for increasing coupling, we expect that the width of our $\phi(2170)$ candidate may thus be reduced. Conversely, including the widths of final-state resonances will probably *increase* the widths of the now too narrow excited ϕ resonances stemming from the confinement spectrum.

Of course, to account for the nonvanishing widths of mesons in the coupled channels is a very difficult problem, since the simple substitution of the here used real masses by the true complex masses will destroy the manifest unitarity of the S matrix. Work is in progress to redefine the S matrix for such cases, so as to enforce its unitarity by construction.

ACKNOWLEDGMENTS

We are indebted to Dr. Kanchan Khemchandani for very useful discussions on the $\phi(2170)$ resonance, and to Professor David Bugg for several helpful comments on the first version of the present paper. This work was supported by the Fundação para a Ciência e a Tecnologia of the Ministério da Ciência, Tecnologia e Ensino Superior of Portugal, under Contract No. CERN/FP/83502/2008.

[1] B. Aubert *et al.* (*BABAR* Collaboration), Phys. Rev. D **74**, 091103 (2006).
[2] M. Ablikim *et al.* (BES Collaboration), Phys. Rev. Lett. **100**, 102003 (2008).
[3] C. Amsler *et al.* (Particle Data Group), Phys. Lett. B **667**, 1 (2008).
[4] C. P. Shen *et al.* (Belle Collaboration), Phys. Rev. D **80**, 031101(R) (2009).
[5] G. J. Ding and M. L. Yan, Phys. Lett. B **650**, 390 (2007).
[6] G. J. Ding and M. L. Yan, Phys. Lett. B **657**, 49 (2007).
[7] Z. G. Wang, Nucl. Phys. **A791**, 106 (2007).
[8] H. X. Chen, X. Liu, A. Hosaka, and S. L. Zhu, Phys. Rev. D **78**, 034012 (2008).
[9] M. Napsuciale, E. Oset, K. Sasaki, and C. A. Vaquera-Araujo, Phys. Rev. D **76**, 074012 (2007).
[10] A. Martinez Torres, K. P. Khemchandani, L. S. Geng, M. Napsuciale, and E. Oset, Phys. Rev. D **78**, 074031 (2008).
[11] S. L. Zhu, Int. J. Mod. Phys. E **17**, 283 (2008).
[12] E. van Beveren and G. Rupp, Int. J. Theor. Phys. Group Theory Nonlinear Opt. **11**, 179 (2006).
[13] E. van Beveren and G. Rupp, Ann. Phys. (N.Y.) **324**, 1620 (2009).
[14] G. Rupp, S. Coito, and E. van Beveren, arXiv:0905.3308 [Acta Phys. Pol. B Proc. Suppl. (to be published)].
[15] E. van Beveren and G. Rupp, Phys. Rev. Lett. **91**, 012003 (2003).
[16] E. van Beveren, D. V. Bugg, F. Kleefeld, and G. Rupp, Phys. Lett. B **641**, 265 (2006).
[17] E. van Beveren and G. Rupp, Eur. Phys. J. A **31**, 468 (2007).
[18] E. van Beveren and G. Rupp, Phys. Rev. Lett. **97**, 202001 (2006).
[19] S. Coito, G. Rupp, and E. van Beveren, arXiv:0905.3302 [Acta Phys. Pol. B Proc. Suppl. (to be published)]. Note that in this study restricted to the $^3S_1$ $s\bar{s}$ channel the dependence of the coupling constants on the radial quantum number n was not properly normalized, resulting in too large coupled-channel effects for the higher excited states.
[20] E. van Beveren, Z. Phys. C **21**, 291 (1984).
[21] E. van Beveren, G. Rupp, T. A. Rijken, and C. Dullemond, Phys. Rev. D **27**, 1527 (1983).
[22] R. Delbourgo and M. D. Scadron, Int. J. Mod. Phys. A **13**, 657 (1998).
[23] Yu. S. Surovtsev and P. Bydzovsky, Nucl. Phys. **A807**, 145 (2008).
[24] N. N. Achasov and A. A. Kozhevnikov, Phys. Rev. D **57**, 4334 (1998); Phys. At. Nucl. **60**, 2029 (1997) [Yad Fiz. **60**, 2212 (1997)].
[25] R. R. Akhmetshin *et al.*, Phys. Lett. B **551**, 27 (2003).
[26] E. van Beveren, C. Dullemond, and G. Rupp, Phys. Rev. D **21**, 772 (1980); **22**, 787(E) (1980).
[27] E. van Beveren and G. Rupp, Ann. Phys. (N.Y.) **323**, 1215 (2008).